Macromolecules
Cite This: Macromolecules XXXX, XXX, XXX–XXX
Article
pubs.acs.org/Macromolecules

Controlled Synthesis and Supramolecular Organization of Conjugated Star-Shaped Polymers

Marie-Paule Van Den Eede,[†] Julien De Winter,[‡] Pascal Gerbaux,[‡] Joan Teyssandier,[§] Steven De Feyter,[§] Cédric Van Goethem,[∥] Ivo F. J. Vankelecom,[∥] and Guy Koeckelberghs*[,†]

[†]Laboratory for Polymer Synthesis, Department of Chemistry, KU Leuven, Celestijnenlaan 200F, B-3001 Heverlee, Belgium
[‡]Organic Synthesis and Mass Spectrometry Laboratory, Interdisciplinary Center for Mass Spectrometry, University of Mons-UMONS, 23 Place du Parc, 7000 Mons, Belgium
[§]Division of Molecular Imaging and Photonics, Department of Chemistry, KU Leuven, Celestijnenlaan 200F, B-3001 Heverlee, Belgium
[∥]Center for Surface Chemistry and Catalysis, Department of Microbial and Molecular Systems, KU Leuven, Celestijnenlaan 200F, B-3001 Heverlee, Belgium

Supporting Information

ABSTRACT: Through the incorporation of chiral and achiral poly(3-alkylthiophenes) (P3ATs) into a star-shaped system, a well-defined supramolecular organization is obtained lacking the unfavorable linear lamellar structure typically obtained for P3AT. Through the combination of a controlled chain-growth polymerization and efficient postpolymerization and click reactions, well-defined star-shaped P3ATs with a low dispersity of 1.1 were obtained. The combination of UV−vis, circular dichroism (CD), atomic force microscopy (AFM), and transmission electron microscopy (TEM) measurements showed the formation of a strong (chiral) supramolecular organization into fibers, different and stronger than those obtained with the linear P3ATs. The fact that the width of the fibers is in good agreement with the width of a single star-shaped P3AT excludes the formation of a linear lamellar structure. Furthermore, the particular supramolecular organization of the star-shaped polymers, which appears thanks to the precision polymer synthesis, triggers properties of the arms of the star-shaped molecule that are not present in the individual arms.

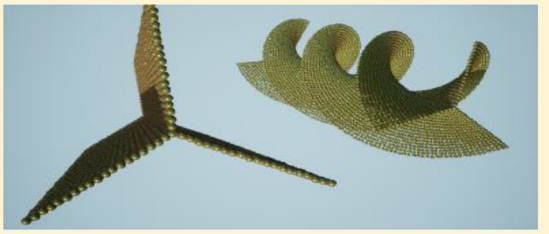

INTRODUCTION

Organic optoelectronics have gained a great deal of attention in the past decade due to the search for renewable and environmentally friendly energy sources. Semiconducting conjugated polymers have been proven to be outstanding materials for these applications due to their lower cost and easier processability into thin films, impressive optoelectronic properties, and the possibility to tune the (low) band gap through chemical modifications.[1−3] P3AT, which is the model polymer for a broad variety of research regarding optoelectronics (e.g., charge transport and film morphology), has already been used in different applications, such as organic field effect transistors (*o*FETs) and organic photovoltaics (*o*PVs).[1,4−9] For these applications it has been well established that the morphology has a significant effect on the charge transfer and consequently on the device performance.[10−13] Aggregation of P3ATs is mainly driven by strong $\pi-\pi$ interactions. Apart from these $\pi-\pi$ interactions also weaker lamellar interactions along the side chains are present (Figure 1). Already different attempts to design P3AT systems with controlled morphologies have been made (e.g., introduction of unsubstituted thiophene units and copolymerization of thiophene units with different side-chain lengths); however, obtaining well-ordered morphologies remains difficult due to the fast formation of the weaker lamellar structure.[1,7,14−21] Furthermore, a fast interchain and intrachain charge transport is possible between the π-stacked P3ATs and along the P3AT backbone respectively, while only a slow interchain charge transport is present in the lamellar structure.[22]

Ponomarenko et al. prepared star-shaped oligothiophenes as semiconducting materials with better film-forming properties for *o*FETs.[23] By changing the molecular structure of these star-shaped oligothiophenes, they were able to create more ordered morphologies. In this research we aim to develop a stronger ordered morphology of polymers by incorporating linear P3AT into a well-defined star-shaped structure with a low dispersity. In order to obtain these well-defined star-shaped P3ATs, the advantages of a controlled chain-growth polymerization of P3AT and efficient postpolymerization and click reactions are combined in a new synthetic pathway. Apart from an achiral system, also a chiral star-shaped system is formed in order to

Received: August 17, 2018
Revised: October 8, 2018

DOI: 10.1021/acs.macromol.8b01777
Macromolecules XXXX, XXX, XXX–XXX

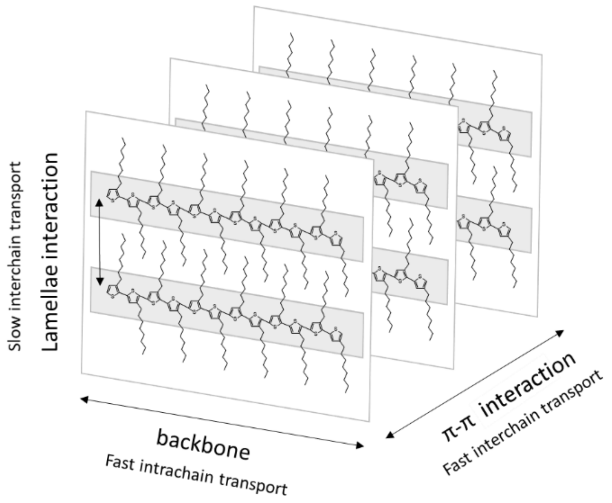

Figure 1. Schematic visualization of the π-stacking of P3ATs.

create a system which is able to organize in a chiral way and to visualize the aggregation with CD.

RESULTS AND DISCUSSION

Design of the Star-Shaped Polymers. Three main methods exist to obtain star-shaped polymers.[24,25] The first, the "coupling-onto" strategy, relies on the coupling of end-functionalized polymer chains on a central core. This method is especially useful when a controlled polymerization is obtained. The second, or "arm-first" strategy, relies on polymer arm precursors with usually a divinyl compound to form the star-shaped polymer with a cross-linked core. However, broad molar mass distributions are obtained with this method due to the random distribution of the arms per core during the cross-linking process. The last, more popular method, known as the "core-first" strategy, makes use of a multifunctional initiator at which the different arms start to polymerize. Even though this strategy appears to be the best option, it requires the presence of an extended phenylene spacer between the P3AT arms and the central core.[26,27] Since a structure that is as planar as possible needs to be obtained for this research and the conjugated spacer can result in a distortion in the structure, the "coupling-onto" method has been chosen as a synthetic strategy in order to obtain a core which enables a planar structure. Exploiting the discovery of the living chain-growth polymerization of P3AT, it is possible to obtain polythiophenes with the required low dispersity and controlled molar mass.[28−30] Furthermore, when a chain growth polymerization is initiated by an external functionalized initiator, all chains will bear the functional group.[31,32] With this method, the functional group, which is necessary to attach the polymer arms to the core, will be implemented. In order to attach the polymer arms in an efficient way to the central core, a copper(I)-catalyzed alkyne−azide cycloaddition (Cu(I)AAC) click reaction has been chosen.[33,24] Due to safety reasons and product availability, the polymer chains bear the azide group, while the central core is equipped with three acetylene groups. Since it is not possible to directly introduce the azide group on the polymer due to incompatibility with the Grignard reagent and the fact that azide groups are more stable on polymer molecules in comparison to small organic molecules such as the external initiator, postpolymerization reactions are necessary. Because of reaction of Grignard monomers with H^+ donors, an external initiator with a protected alcohol is

Scheme 1. Schematic Representation of the Synthetic Pathway Performed in Order To Obtain the Star-Shaped Polythiophene Systems

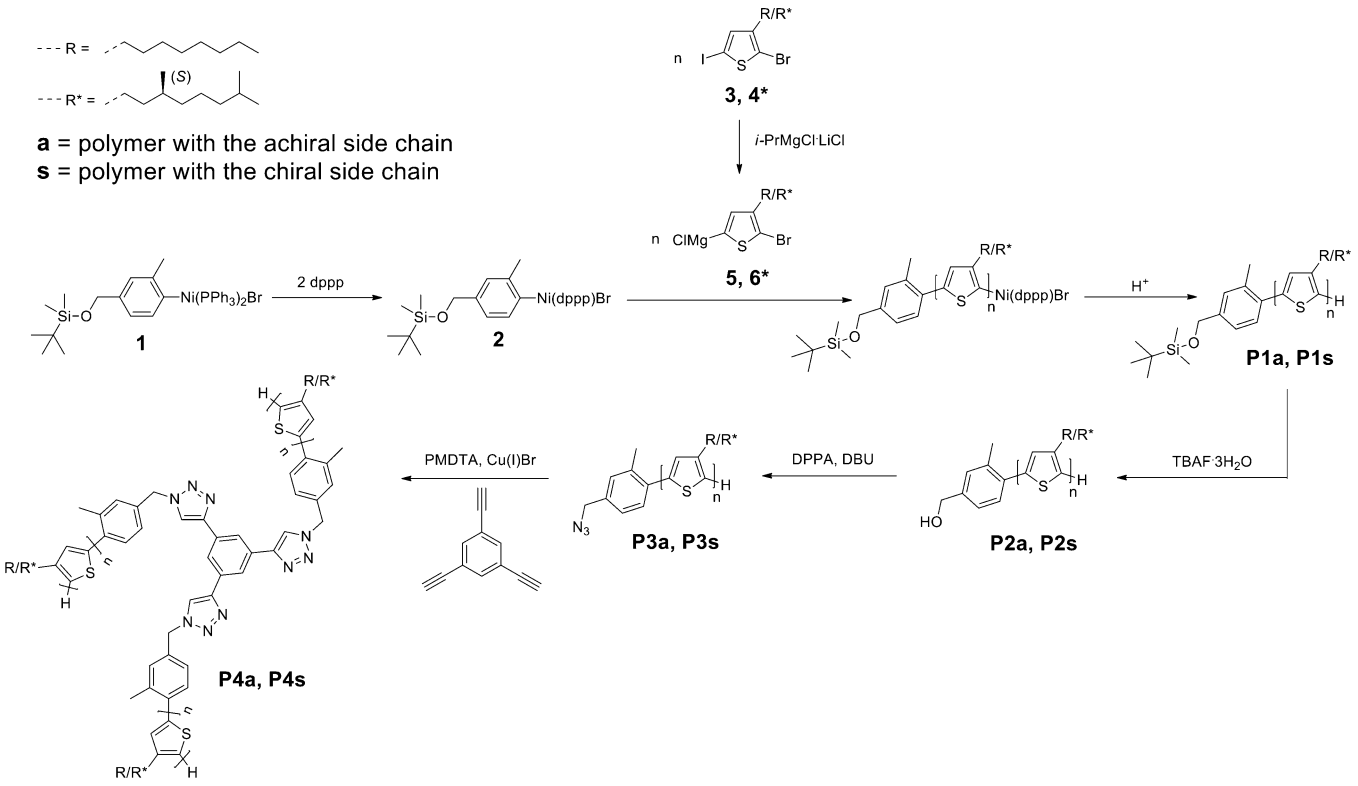

DOI: 10.1021/acs.macromol.8b01777
Macromolecules XXXX, XXX, XXX−XXX

required (Scheme 1). A postpolymerization deprotection and azide formation results in the desired functionalized polymer arms. A last aspect that should be taken into account is the degree of polymerization (DP) of the polymer arms. It has been proven that the polymer chain ends start to fold at a certain DP, which finally can result in the disruption of the supramolecular organization. On the other hand, if the DP is too low, the polymer chains will have difficulties to stack. In order to avoid these two undesired phenomena, a DP of 18 is chosen. Apart from the achiral system, also a chiral star-shaped polymer is created. The latter allows the creation of a system that organizes in a chiral way and the visualization of the aggregation with CD. The chosen synthetic pathway is visualized in Scheme 1.

Synthesis of the Precursor Initiator. The external precursor initiator was prepared in dry toluene by mixing $Ni(PPh_3)_4$ with 1-bromo-2-methyl-4-[(*tert*-butyl)-dimethylsilyloxymethyl]benzene (page S5 in the Supporting Information).[34]

Synthesis of the Polymers. All polymers were synthesized using a Ni(dppp) (dppp = bis(diphenylphosphino)-propane) mediated Kumada catalyst transfer condensative polymerization (KCTCP) (Scheme 1). Prior to the polymerization, a Grignard metathesis (GRIM) reaction of the 3-alkyl-2-bromo-5-iodothiophene precursor monomers **3** and **4*** resulted in the corresponding achiral monomer **5** and *S*-chiral monomer **6***.[31] Since monomers **5** and **6*** contain a Grignard functionality, a protected alcohol function on the external initiator was required during the polymerization.[34] The external precursor initiator **1** underwent a ligand exchange with dppp in order to obtain the desired initiator **2**. Exploiting the living nature of the polymerization, the end-functionalized achiral polymer **P1a** and *S*-chiral polymer **P1s** were obtained by initiating the polymerization with the external initiator **2**. Since the polymerization is controlled, the DP was fixed on 18 units by adapting the monomer to initiator ratio. The polymerizations were terminated with a 1 M acidified (HCl) THF solution, in order to prevent disproportionation.[30] During this last step some alcohol functions were deprotected. This does not pose any problem, since the next postpolymerization step consists of the deprotection of **P1a** and **P1s**. GPC measurement (Figure S47) of the polymers **P1a** and **P1s** in THF toward polystyrene standards was the first indication of a successful polymerization. For both polymers a low dispersity ($Đ$) of 1.1 was obtained (Table 1).

Although GPC gives an estimation of the molar mass, the use of polystyrene standards inevitably results in a deviation of this molar mass. Since P3ATs are more rigid, an overestimation is obtained. Nonetheless, ^{1}H NMR makes it possible to determine the DP via end-group quantification. This was done via the assignment of separated signals originating from the internal monomer units and the *o*-tolyl protons of the end group (Figure 2). The number-average molar mass ($\bar{M}_n$) and $Đ$ obtained with GPC and the DP for polymer **P1a** and **P1s** obtained with ^{1}H NMR are shown in Table 1. The overestimation of the molar mass obtained with GPC is in accordance with the size-exclusion quantification.[35,36] MALDI-ToF was used in order to confirm that polymers **P1a** and **P1s** are mainly initiated by the tolyl derivative, confirming that the ^{1}H NMR calculations are correct (page S12 in the Supporting Information).

Postpolymerization Reactions. Three postpolymerization steps were performed according to literature procedure (pages S6–S8 in the Supporting Information).[33] All postpolymerization reactions were monitored by ^{1}H NMR spectroscopy. More specifically, the shift of the signal of the CH_2 protons next to the functional group was followed (Figure 3). Furthermore, MALDI-ToF measurements were taken after each polymerization and postpolymerization step (pages S13 and S14 in the Supporting Information). All postpolymerization reactions were shown to be almost quantitative. The first step consists of the deprotection of the silyl-protected alcohol function of **P1a** and **P1s** with an excess of TBAF·3H_2O. Upon formation of **P2a** and **P2s**, a small shift of the signal of the CH_2 protons from 4.75 to 4.70 ppm can be noticed (Figure 3). In a second step, the alcohol group was transformed into an azide

Table 1. Overview of the Results of GPC ($\bar{M}_n$, $Đ$) and ^{1}H NMR

Schematic representation	Polymer	$\bar{M}_n$ [a] (kg/mol)	n [a]	$Đ$ [a]	n [b]
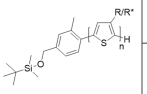	**P1a**	4.8	23	1.1	18
	P1s	5.7	24	1.1	18
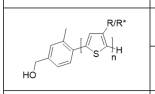	**P2a**	4.6	23	1.1	18
	P2s	5.5	24	1.1	18
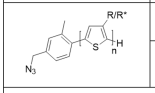	**P3a**	4.7	23	1.1	18
	P3s	5.7	24	1.1	18
For **PXa** (X = 1, 2, 3), ---R = 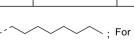 ; For **PXs** (X = 1, 2, 3), ---R* = 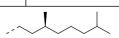					

[a]Determined by GPC. [b]Determined by ^{1}H NMR.

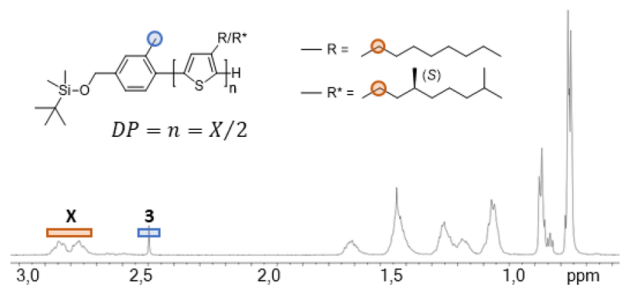

Figure 2. Assignment of the separated signals originating from the internal monomer units and the *o*-tolyl protons of the end group for the determination of the degree of polymerization.

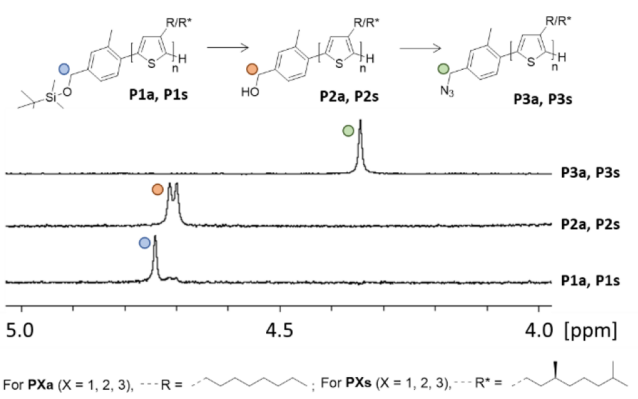

Figure 3. ^{1}H NMR spectra of postpolymerization of **P1a**, **P1s**, **P2a**, **P2s**, **P3a**, and **P3s**.

DOI: 10.1021/acs.macromol.8b01777
Macromolecules XXXX, XXX, XXX−XXX

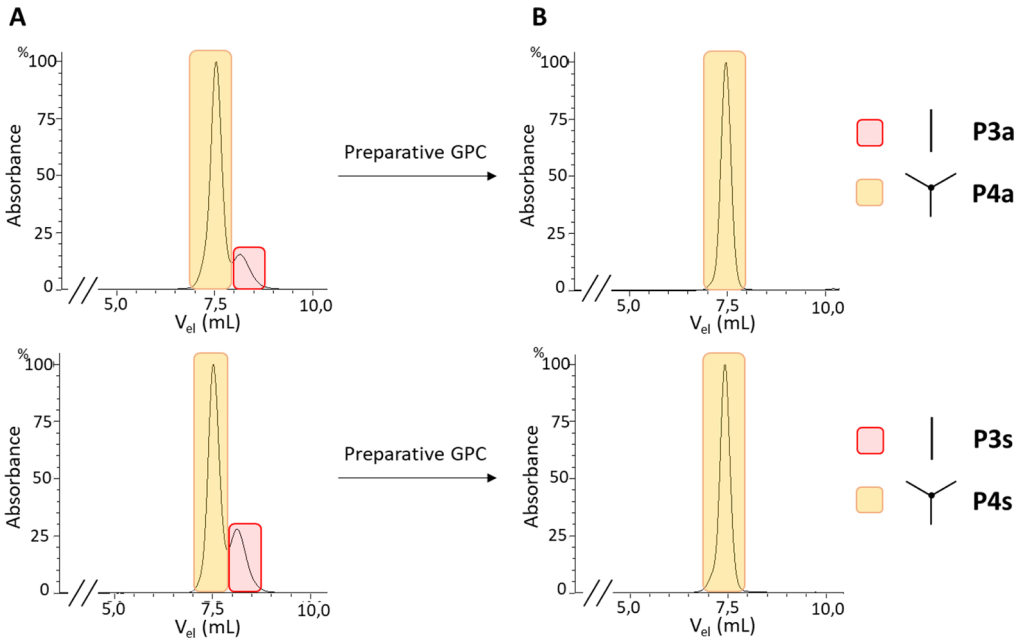

Figure 4. GPC analysis of (A) **P3a** and **P3s** after a click reaction and (B) **P4a** and **P4s** after preparative GPC.

group, by reacting **P2a** and **P2s** with diphenylphosphoryl azide (DPPA) and 1,8-diazabicycloundec-7-ene (DBU). During the conversion of **P2a** and **P2s** into **P3a** and **P3s**, respectively, a clear shift of the same signal of the CH_2 protons takes place from 4.70 to 4.35 ppm (Figure 3). In order to confirm that nothing unexpected happened with the polymers during these postpolymerization steps, GPC measurements were performed after each step (Table 1). For all polymers monomodal peaks with a low dispersity of 1.1 were obtained (pages S35 and S36 in the Supporting Information).

Click Reaction. In a last step, the azide-functionalized *S*-chiral and achiral P3AT arms were attached to the central core via a Cu(I)AAC click reaction. **P3a** and **P3s** were attached to the core, using *N,N,N′,N″,N″*-pentamethyldiethylenetriamine (PMDTA) and $Cu^{I}Br$ (Scheme 1). Importantly, a small excess of polymer **P3a** or **P3s** was used with respect to the core, as it is easier to purify a mixture of the desired tricoupled product and free **P3a** or **P3s** than to purify a mixture of tricoupled and dicoupled product. The click reaction was monitored by GPC, and the end result is shown in Figure 4A. Since it was not possible to remove all remaining **P3a** or **P3s** with Soxhlet extraction, preparative GPC was performed. The GPC measurements of this purification step are shown in Figure 4B.

After purification, ^{1}H NMR spectra were taken in order to validate the success of the click reaction and removal of free **P3a** and **P3s**.[33] As shown in Figure 5, the signal of the CH_2 protons next to the functional group of the initiator moved from 4.70 to 5.58 ppm and no signal at 4.70 ppm remained in the ^{1}H NMR spectrum of **P4a** and **P4s**. In addition, MALDI-ToF analyses of **P4a** and **P4s** were performed in order to prove the efficiency of the Cu(I)AAC click reaction. Indeed, as presented in Figure 6, **P4a** and **P4s** are characterized by a distribution almost 3 times higher in mass than the precursor confirming the formation of the 3 armed star polymer. Moreover, a comparison with the theoretical isotopic model proved the formation of the expected structure (Supporting Information page S15).

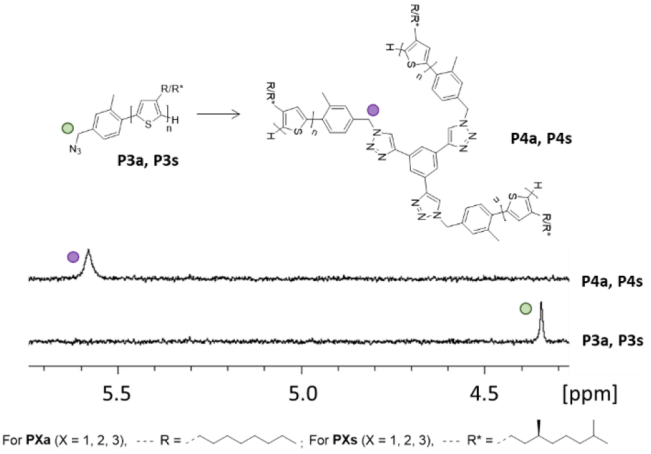

Figure 5. ^{1}H NMR spectra of **P3a** and **P3s** and click reaction to form **P4a** and **P4s**.

UV–Vis and CD Measurements. Polymers **P4a** and **P4s** were subjected to a solvatochromism experiment. By also measuring **P3a** and **P3s**, we could determine the influence of the star-shaped nature of **P4a** and **P4s** on the supramolecular aggregation. All polymers were dissolved in chloroform ($CHCl_3$), which is a typical, good solvent for P3ATs. Under this condition, the polymers adopt a achiral random coil-like structure and no CD signal is measured. In a next step, methanol (MeOH), a nonsolvent, is added incrementally. At a critical amount of added nonsolvent, polymer chains start to stack. This can occur in an achiral way as well as in a chiral way if chiral side chains are present. In the case of achiral side chains, only a red shift of the P3AT band and fine structure is obtained in the UV–vis spectrum, while no CD signal is seen. On the other hand, if chiral side chains are present, a bisignate Cotton effect is obtained in the CD spectrum, as a result of the formation of a chiral supramolecular structure. Since the intensity (and sign and shape) of the CD signal can depend on the circumstances under which methanol is added, all samples were measured at room temperature and methanol was added

DOI: 10.1021/acs.macromol.8b01777
Macromolecules XXXX, XXX, XXX–XXX

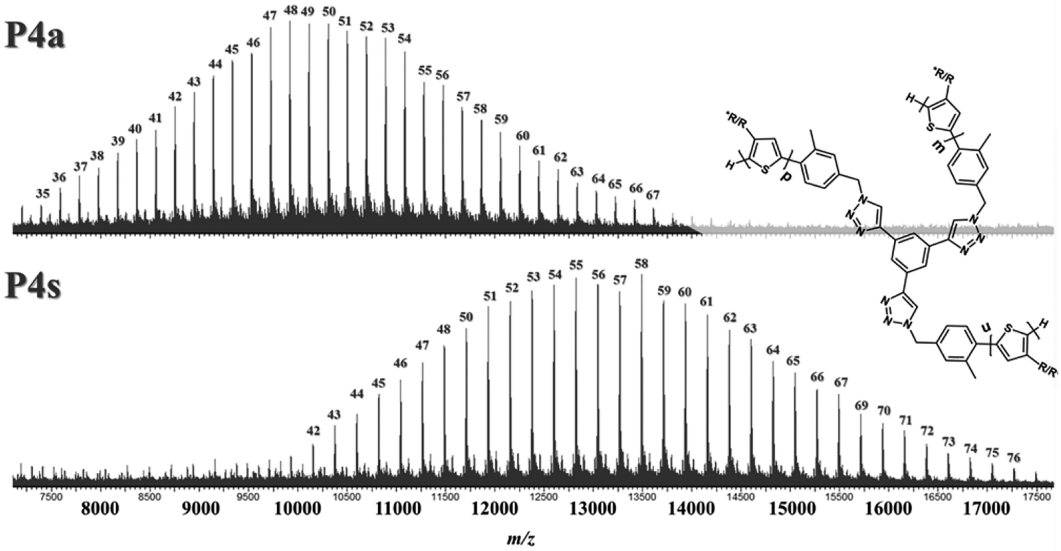

Figure 6. MALDI-ToF spectra of **P4a** and **P4s**. The number on the top of each signal corresponds to the total number of monomer units ($n + m + p$). The center of the distribution for **P4a** is 50 and that for **P4s** is 55−57, consistent with the expected value, which should be 54 (18 × 3).

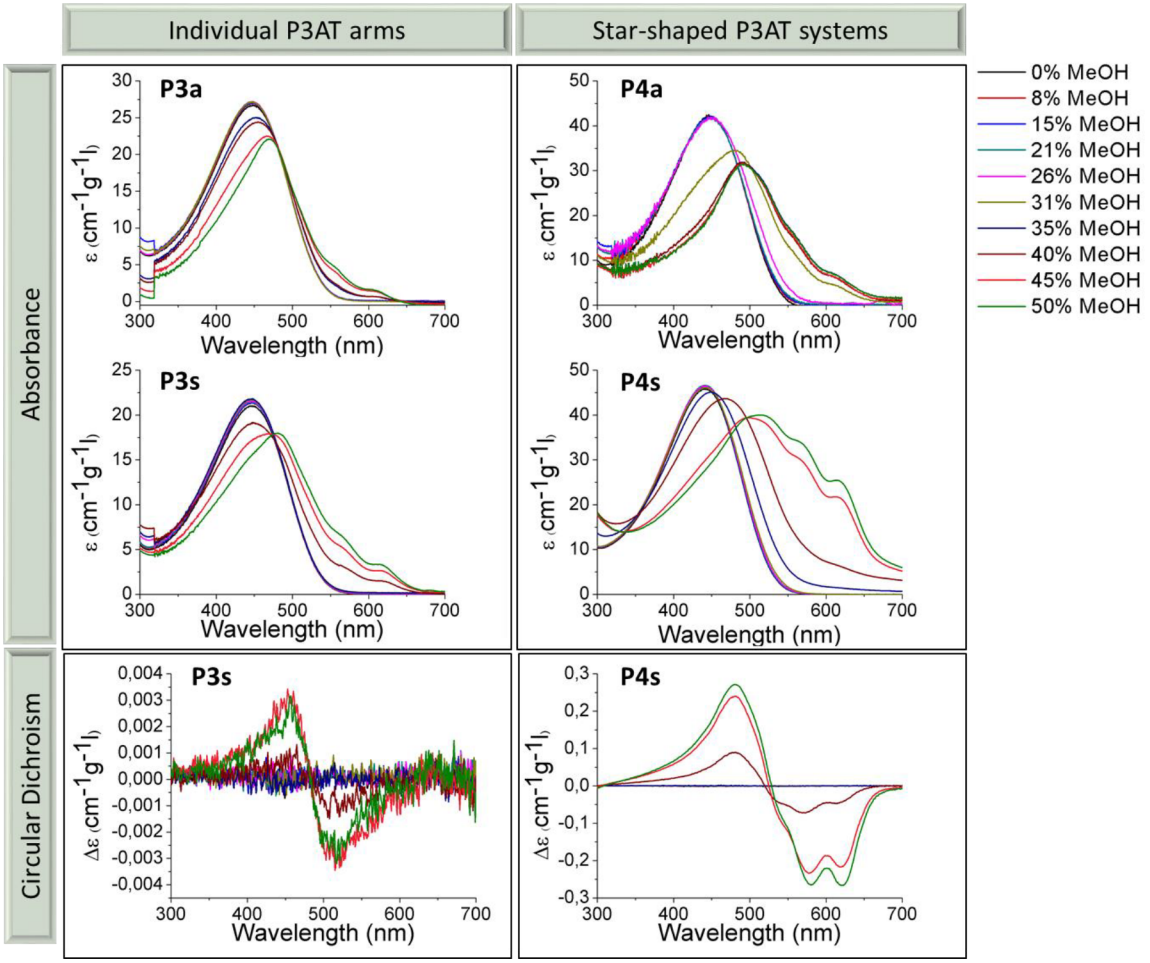

Figure 7. UV−vis spectra (top) and CD spectra (bottom) of **P3a** and **P3s** (left) and **P4a** and **P4s** (right).

at a constant speed of 0.20 mL/min using a syringe pump. All UV−vis and CD spectra can be found in pages S16−S19 in the Supporting Information. As shown in the UV−vis spectrum of **P3a** (Figure 7), some aggregation took place at a methanol content of 42%, visualized by a red shift from 430 to 460 nm and the appearance of fine structure. The polymer chains of the individual arms start to aggregate only at high nonsolvent content, and the supramolecular organization is limited, as the intensity of the additional peaks is small. This can be explained by the presence of the *o*-tolyl end group in combination with

DOI: 10.1021/acs.macromol.8b01777
Macromolecules XXXX, XXX, XXX−XXX

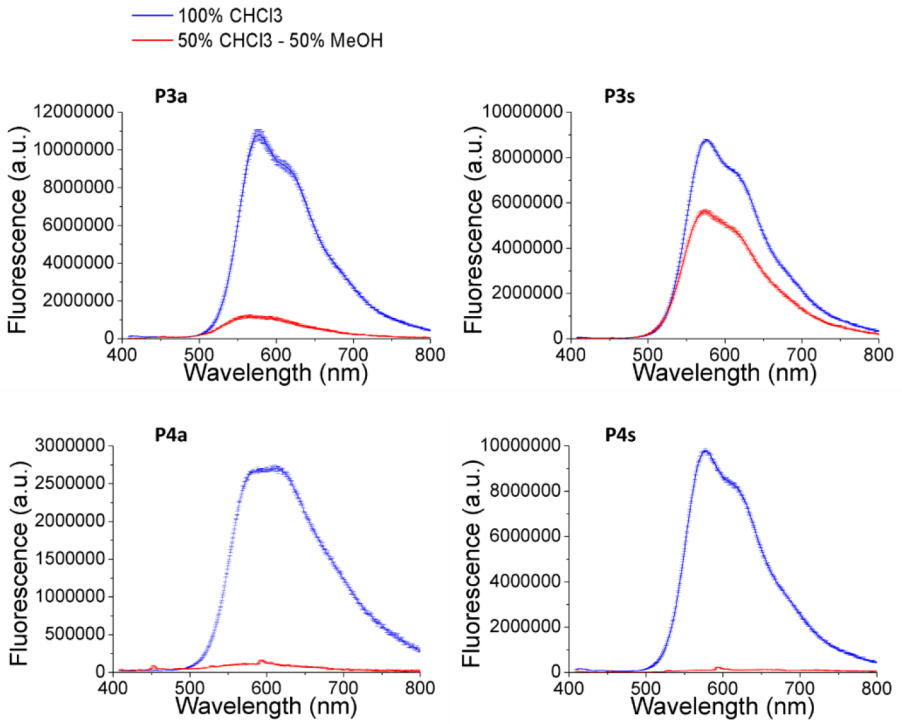

Figure 8. Fluorescence spectra of **P3a**, **P3s**, **P4a**, and **P4s** in pure chloroform and in a chloroform/MeOH 50/50 mixture.

the limited molar mass of the polymers. High molar masses lead to more supramolecular organization. In addition for **P3s**, the polymer chains only start to aggregate around a methanol content of 40% (Figure 7). In contrast to **P3a**, a red shift is visualized from 430 to 490 nm and more fine structure is visible. Since **P3s** may organize in a chiral way, also CD was measured, as shown in Figure 7. From these spectra it is clear that the polymer chains have some difficulty in aggregating, resulting in a small CD signal visible from 40% of methanol. This is in line with the results obtained with UV−vis spectroscopy. For both polymers **P3a** and **P3s**, we can conclude that most of the polymer chains do not organize. More in particular, even at a methanol content of 50%, a clear signal around 430 nm remains visible. From the UV−vis spectra of the achiral star-shaped **P4a** (Figure 7), it is clear that the polymer chains start to stack at a methanol content of 35%. In contrast to **P3a**, the polymer chains start to stack at a lower content of methanol and a much more pronounced red shift of the P3AT band is visible from 430 to 490 nm. For the chiral star-shaped **P4s**, UV−vis and CD analyses were performed (Figure 7). In the UV−vis spectra a stepwise red shift, starting from 35% of methanol, is visible from 430 to 525 nm which is much more pronounced than for the parent arms. Furthermore, a more defined fine structure is visible. These remarkable results are also confirmed by CD analysis. In contrast to linear **P3s**, a high (negative) CD signal is visible, which is much higher than that obtained for linear P3AT systems. In order to compare, the $g_{abs,max}$ ($=\Delta\varepsilon/\varepsilon$) values were calculated. Whereas a value of −0.00026 was obtained for **P3s**, **P4s** resulted in a value of −0.01, which is almost 2 orders of magnitude larger than that for **P3s**. These results are remarkable since, even if a perfect planarization of all arms occurs, there is still no conjugation present between the arms, due to the presence of two meta linkages (triazole and central phenyl) and the presence of two sp^3-hybridized carbon atoms between two arms. Hence, it must be concluded that this much more pronounced supramolecular organization is not due to the higher conjugation length but to the particular supramolecular organization of the star-shaped polymers which triggers properties of the arms that are not present in the individual arms.

Fluorescence Spectroscopy. Further investigation of the polymer aggregation in solution was done via fluorescence spectroscopy. The fluorescence of polymers **P3a**, **P3s**, **P4a**, and **P4s** was measured in pure chloroform, in which the polymer chains are molecularly dissolved, and in a 50/50 mixture of $CHCl_3$/MeOH, in which the polymer chains are mostly aggregated, in accordance with the UV−vis spectra. The emission spectra were recorded from 410 to 800 nm, after excitation at 400 nm. For each sample, 3 × 10 scans were taken. With these results the mean values and standard deviations of the absorption-corrected fluorescence spectra have been calculated and plotted as shown in Figure 8 (all spectra are given in pages S20−S26 in the Supporting Information). On going from a good solvent to a poor solvent mixture, the intensities of **P3a** and **P3s** drop by factors of 11 and 1.5, respectively, while for **P4a** and **P4s** the intensities drop by factors of 30 and 50, respectively. This difference between the linear and star-shaped polymers can be explained by the difference in aggregation ability. More in particular, the two linear P3ATs (**P3a** and **P3s**) are aggregated to a smaller extent, as already demonstrated by the UV−vis and CD measurements. This resulted in a lower quenching of the fluorescence.

DSC Measurements. The properties of the different linear and star-shaped polymers in the solid state were studied by differential scanning calorimetry (DSC). The thermal properties of **P3a**, **P3s**, **P4a**, and **P4s** were studied by recording DSC thermograms (pages S26−S28 in the Supporting Information). For all polymers crystallization peaks were observed, as expected from the UV−vis and CD measurements. As expected, lower T_m values are obtained for the chiral structures.

DOI: 10.1021/acs.macromol.8b01777
Macromolecules XXXX, XXX, XXX−XXX

The T_m values of **P3a** and **P4a**, **P3s**, and **P4s** are approximately the same.

AFM Measurements. In order to obtain more information about the supramolecular organization, AFM measurements on thin film samples were performed. AFM imaging was performed on films obtained by drop-casting of diluted (0.1 mg.ml^{-1}) solutions of the four different polymers on graphite. The star-shaped polymers **P4a** and **P4s** could both form fibrous structures after drop-casting of solutions in chloroform (Figure 9b,d), while no ordered structures were observed from

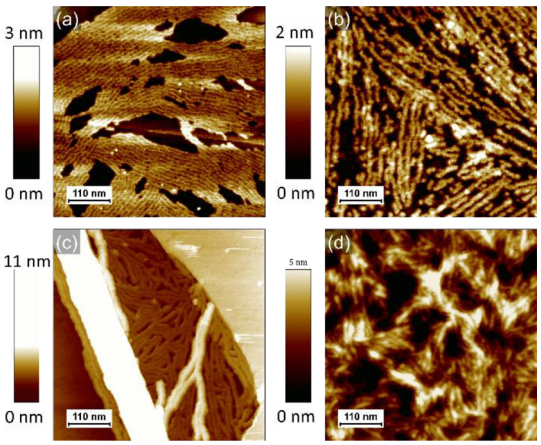

Figure 9. AFM topography images of dry films of **P3a** (a), **P4a** (b), **P3s** (c), and **P4s** (d) on graphite. Films of **P3a** and **P3s** were drop-casted from 0.1 mg mL^{-1} solutions in toluene, and films of **P4a** and **P4s** were prepared from solutions of the same concentration in chloroform.

this solvent for the two azide polymers **P3a** and **P3s** (pages S28–S33 in the Supporting Information). This observation confirms qualitatively the tendency revealed by UV–vis and CD measurements in solution of the star-shaped polymers to reach a higher degree of organization in comparison to the linear polymers. Nevertheless, when they were prepared from toluene solutions, films of **P3a** and **P3s** did exhibit fibers (Figure 9a,c), which allows structural comparison between the linear and star-shaped polymers. The films can be composed of one or several layers of the polymers (see the Supporting Information for more details). The lamellar structures shown in Figure 9 are typical of poly(3-hexylthiophene) films.[37,38,1] These features are caused by the π stacking of the polymer backbone perpendicular to the axis of the fibers. As a consequence, the width of the fibers can serve as an estimation of the length of the polymer chains. For the azide polymers, those widths (9.6 ± 0.8 nm for **P3a** and 10.1 ± 1.4 nm for **P3s**) are in good agreement with the expected length of the planar chain. The fibers formed by the star-shaped polymers are slightly wider (14.8 ± 2.6 nm for **P4a** and 14.8 ± 1.4 nm for **P4s**), suggesting a different internal organization. This slight difference is in qualitative agreement with the proposed structure of aggregates in solution.

With the value obtained for the arms (**P3a** and **P3s**), the expected value for the width of the fiber formed by the star-shaped polymer **P4a** and **P4s**, was calculated (page S34 in the Supporting Information). The obtained values of approximately 15.0 nm for **P4a** and 15.8 nm for **P4s**, taking into account the margin of error, are in good agreement with the experimentally obtained values of 14.8 ± 2.6 and 14.8 ± 1.4 nm, respectively. If two arms of the star-shaped system align at an angle of 180°, which would enable the formation of the possible lamellar structure, a value of at least twice the width of its individual arms should be measured. However, this is not the case. AFM therefore demonstrates that the fibrils are constituted of stacks of single, star-shaped polymers.

TEM Visualization. Finally, TEM was performed on the chiral star-shaped P3AT **P4s**. The sample was prepared from a diluted chloroform solution. A representative TEM picture is shown in page S35 in the Supporting Information. A linear structure with a width of ∼14 nm is found, which is in line with the AFM data.

When the results obtained by UV–vis and CD spectroscopy (the formation of a highly ordered structure) as well as AFM and TEM (formation of fibers with a width of approximately 14 nm) are combined, a particular supramolecular organization of the star-shaped macromolecules into more organized fibers is obtained.

CONCLUSION

We were able to synthesize both an achiral (**P4a**) and chiral (**P4s**) star-shaped P3AT with a low dispersity of 1.1. The arms of both systems have an average DP of 18. UV–vis and CD measurements showed a clear supramolecular aggregation for both of the star-shaped polymers, much stronger than the aggregation obtained for the linear P3ATs. For the chiral star a high CD signal was also obtained, indicating that a highly organized chiral supramolecular aggregation is formed. AFM measurements on both star-shaped P3ATs and linear P3ATs were performed. These measurements confirm that the star-shaped P3ATs organize in a supramolecular way into fibers. The width obtained for the fibers is in good agreement with the calculations of the width of the star-shaped P3ATs. These results are remarkable since, even if a perfect planarization of all arms occurs, there is still no conjugation present between the arms, due to the presence of two meta linkages (triazole and central phenyl) and the presence of two sp^3-hybridized carbon atoms between two arms. Hence, it must be concluded that the particular supramolecular organization of the star-shaped polymers, which appears thanks to the precision polymer synthesis, triggers properties of the arms that are not present in the individual arms.

ASSOCIATED CONTENT

Supporting Information

The Supporting Information is available free of charge on the ACS Publications website at DOI: 10.1021/acs.macromol.8b01777.

Instrumentation used and experimental details as well as ^{1}H NMR, MALDI-ToF, UV–vis, CD, fluorescence, DSC, AFM, TE,M and GPC results (PDF)

AUTHOR INFORMATION

Corresponding Author

*E-mail for G.K.: guy.koeckelberghs@kuleuven.be.

ORCID

Julien De Winter: 0000-0003-3429-5911
Joan Teyssandier: 0000-0003-4369-0542
Steven De Feyter: 0000-0002-0909-9292
Cédric Van Goethem: 0000-0003-2218-2143
Guy Koeckelberghs: 0000-0003-1412-8454

DOI: 10.1021/acs.macromol.8b01777
Macromolecules XXXX, XXX, XXX–XXX

Notes

The authors declare no competing financial interest.

■ ACKNOWLEDGMENTS

We are grateful to the Onderzoeksfonds KU Leuven/Research Fund KU Leuven for funding this project. The Hercules Fund is acknowledged for funding the TEM (AKUL/13/19). C.V.G. acknowledges the Flemish Agency for Innovation through Science and Technology (IWT) for a Ph.D. scholarship (No. 141697). The MS laboratory acknowledges the "Fonds de la Recherche Scientifique (FRS-FNRS)" for its contribution to the acquisition of the Waters QToF Premier instrument and continuing support. J.T. and S.D.F. are grateful to the Belgian Federal Science Policy Office (IAP-7/05), the Fund of Scientific Research−Flanders (FWO), and ERC Grant Agreement No. 340324.

■ ABBREVIATIONS

P3AT, poly(3-alkylthiophene); CD, circular dichroism; AFM, atomic force microscopy; TEM, transmission electron microscopy; *o*FET, organic field effect transistor; *o*PV, organic photovoltaic; Cu(I)AAC, copper(I)-catalyzed alkyne−azide cycloaddition; DP, degree of polymerization; dppp, bis-(diphenylphosphino)propane; GRIM, Grignard metathesis; KCTCP, Kumada catalyst transfer condensative polymerization; GPC, gel permeation chromatography; $Đ$, dispersity; $\bar{M}_n$, number-average molar mass; MALDI-ToF, matrix assisted laser desorption/ionization time-of-flight; DPPA, diphenylphosphoryl azide; DBU, 1,8-diazabicycloundec-7-ene; PMDTA, *N,N,N′,N″,N″*-pentamethyldiethylenetriamine; ε, extinction coefficient; $\Delta\varepsilon$, difference in extinction coefficient of left and right circularly polarized light; g_{abs}, anisotropic factor; λ_{max}, wavelength of maximum absorption; MeOH, methanol; THF, tetrahydrofuran; DSC, differential scanning calorimetry; T_m, melting temperature.

■ REFERENCES

(1) Sirringhaus, H.; Brown, P. J.; Friend, R. H.; Nielsen, M. M.; Bechgaard, K.; Langeveld-Voss, B. M. W.; Spiering, A. J. H.; Janssen, R. A. J.; Meijer, E. W.; Herwig, P.; et al. Two-Dimensional Charge Transport in Self-Organized, High-Mobility Conjugated Polymers. *Nature* **1999**, *401* (6754), 685−688.

(2) Sirringhaus, H.; Kawase, T.; Friend, R. H.; Shimoda, T.; Inbasekaran, M.; Wu, W.; Woo, E. P. High-Resolution Inkjet Printing of All- Transistor Circuits. *Science* **2000**, *290*, 2123−2126.

(3) Yan, H.; Chen, Z.; Zheng, Y.; Newman, C.; Quinn, J. R.; Dötz, F.; Kastler, M.; Facchetti, A. A High-Mobility Electron-Transporting Polymer for Printed Transistors. *Nature* **2009**, *457* (7230), 679−686.

(4) Bao, Z.; Dodabalapur, A.; Lovinger, A. J. Soluble and Processable Regioregular poly(3-hexylthiophene) for Thin Film Field-effect Transistor Applications with High Mobility. *Appl. Phys. Lett.* **1996**, *69* (26), 4108−4110.

(5) Spano, F. C. Modeling Disorder in Polymer Aggregates: The Optical Spectroscopy of Regioregular poly(3-Hexylthiophene) Thin Films. *J. Chem. Phys.* **2005**, *122* (23), 234701.

(6) Klauk, H. Organic Thin-Film Transistors. *Chem. Soc. Rev.* **2010**, *39* (7), 2643−2666.

(7) Thompson, B. C.; Fréchet, J. M. J. Polymer-Fullerene Composite Solar Cells. *Angew. Chem., Int. Ed.* **2008**, *47* (1), 58−77.

(8) Cheng, Y. J.; Yang, S. H.; Hsu, C. S. Synthesis of Conjugated Polymers for Organic Solar Cell Applications. *Chem. Rev.* **2009**, *109* (11), 5868−5923.

(9) Nelson, J. Polymer: Fullerene Bulk Heterojunction Solar Cells. *Mater. Today* **2011**, *14* (10), 462−470.

(10) Savenije, T. J.; Kroeze, J. E.; Yang, X.; Loos, J. The Effect of Thermal Treatment on the Morphology and Charge Carrier Dynamics in a Polythiophene-Fullerene Bulk Heterojunction. *Adv. Funct. Mater.* **2005**, *15* (8), 1260−1266.

(11) Nechifor, C. D.; Dorohoi, D. O.; Ciobanu, C. The Influence of Gamma Radiations on Physico-Chemical Properties of Some Polymer Membranes. *Rom. Reports Phys.* **2009**, *54*, 349−359.

(12) Salleo, A. Charge Transport in Polymeric Transistors. *Mater. Today* **2007**, *10* (3), 38−45.

(13) Frost, J. M.; Cheynis, F.; Tuladhar, S. M.; Nelson, J. Influence of Polymer-Blend Morphology on Charge Transport and Photocurrent Generation in Donor-Acceptor Polymer Blends. *Nano Lett.* **2006**, *6* (8), 1674−1681.

(14) Mccullough, R. D.; Lowe, R. D.; Jayaraman, M.; Anderson, D. L. Design, Synthesis, and Control of Conducting Polymer Architectures: Structurally Homogeneous poly(3-Alkylthiophenes). *J. Org. Chem.* **1993**, *58*, 904−912.

(15) Dimitriev, O. P. Effect of Confinement on Photophysical Properties of P3HT Chains in PMMA Matrix. *Nanoscale Res. Lett.* **2017**, *12*, 510.

(16) Xiao, X.; Wang, Z.; Hu, Z.; He, T. Single Crystals of Polythiophene with Different Molecular Conformations Obtained by Tetrahydrofuran Vapor Annealing and Controlling Solvent Evaporation. *J. Phys. Chem. B* **2010**, *114* (22), 7452−7460.

(17) Han, Y.; Guo, Y.; Chang, Y.; Geng, Y.; Su, Z. Chain Folding in Poly(3-Hexylthiophene) Crystals. *Macromolecules* **2014**, *47* (11), 3708−3712.

(18) Mccullough, B. R. D. The Chemistry of Conducting Polythiophenes **. *Adv. Mater.* **1998**, *10* (2), 93−116.

(19) Liu, J.; Sheina, E.; Kowalewski, T.; McCullough, R. D. Tuning the Electrical Conductivity and Self-Assembly of Regioregular Polythiophene by Block Copolymerization: Nanowire Morphologies in New Di- and Triblock Copolymers. *Angew. Chem., Int. Ed.* **2002**, *41* (2), 329−332.

(20) Zhang, R.; Li, B.; Iovu, M. C.; Jeffries-El, M.; Sauvé, G.; Cooper, J.; Jia, S.; Tristram-Nagle, S.; Smilgies, D. M.; Lambeth, D. N.; McCullough, R. D.; Kowalewski, T. Nanostructure Dependence of Field-Effect Mobility in Regioregular poly(3-Hexylthiophene) Thin Film Field Effect Transistors. *J. Am. Chem. Soc.* **2006**, *128* (11), 3480−3481.

(21) Wu, Z.; Petzold, A.; Henze, T.; Thurn-Albrecht, T.; Lohwasser, R. H.; Sommer, M.; Thelakkat, M. Temperature and Molecular Weight Dependent Hierarchical Equilibrium Structures in Semiconducting poly(3-Hexylthiophene). *Macromolecules* **2010**, *43* (10), 4646−4653.

(22) Ludwigs, S. *P3HT Revisited − From Molecular Scale to Solar Cell Devices*; Springer: Berlin Heidelberg, 2014; Vol. *265*.

(23) Ponomarenko, S. A.; Kirchmeyer, S.; Elschner, A.; Huisman, B. H.; Karbach, A.; Drechsler, D. Star-Shaped Oligothiophenes for Solution-Processible Organic Field-Effect Transistors. *Adv. Funct. Mater.* **2003**, *13* (8), 591−596.

(24) Altintas, O.; Vogt, A. P.; Barner-Kowollik, C.; Tunca, U. Constructing Star Polymersvia Modular Ligation Strategies. *Polym. Chem.* **2012**, *3* (1), 34−45.

(25) Hadjichristidis, N.; Pitsikalis, M.; Pispas, S.; Iatrou, H. Polymers with Complex Architecture by Living Anionic Polymerization. *Chem. Rev.* **2001**, *101* (12), 3747−3792.

(26) Senkovskyy, V.; Beryozkina, T.; Bocharova, V.; Tkachov, R.; Komber, H.; Lederer, A.; Stamm, M.; Severin, N.; Rabe, J. P.; Kiriy, A. A Core-First Preparation of poly(3-Alkylthiophene) Stars. *Macromol. Symp.* **2010**, *291−292* (1), 17−25.

(27) Yuan, M.; Okamoto, K.; Bronstein, H. A.; Luscombe, C. K. Constructing Regioregular Star poly(3-Hexylthiophene) via Externally Initiated Kumada Catalyst-Transfer Polycondensation. *ACS Macro Lett.* **2012**, *1* (3), 392−395.

(28) Sheina, E. E.; Liu, J.; Lovu, M. C.; Laird, D. W.; McCullough, R. D. Chain Growth Mechanism for Regioregular Nickel-Initiated Cross-Coupling Polymerizations. *Macromolecules* **2004**, *37* (10), 3526−3528.

DOI: 10.1021/acs.macromol.8b01777
Macromolecules XXXX, XXX, XXX−XXX

(29) Jeffries-EL, M.; Sauvé, G.; McCullough, R. D. In-Situ End-Group Functionalization of Regioregular poly(3-Alkylthiophene) Using the Grignard Metathesis Polymerization Method. *Adv. Mater.* **2004**, *16* (12), 1017−1019.
(30) Miyakoshi, R.; Yokoyama, A.; Yokozawa, T. Synthesis of poly(3-Hexylthiophene) with a Narrower Polydispersity. *Macromol. Rapid Commun.* **2004**, *25* (19), 1663−1666.
(31) Verswyvel, M.; Monnaie, F.; Koeckelberghs, G. AB Block copoly(3-Alkylthiophenes): Synthesis and Chiroptical Behavior. *Macromolecules* **2011**, *44* (24), 9489−9498.
(32) Monnaie, F.; Brullot, W.; Verbiest, T.; De Winter, J.; Gerbaux, P.; Smeets, A.; Koeckelberghs, G. Synthesis of End-Group Functionalized P3HT: General Protocol for P3HT/nanoparticle Hybrids. *Macromolecules* **2013**, *46* (21), 8500−8508.
(33) Monnaie, F.; Ceunen, W.; De Winter, J.; Gerbaux, P.; Cocchi, V.; Salatelli, E.; Koeckelberghs, G. Synthesis and Transfer of Chirality in Supramolecular Hydrogen Bonded Conjugated Diblock Copolymers. *Macromolecules* **2015**, *48* (1), 90−98.
(34) Smeets, A.; Van Den Bergh, K.; De Winter, J.; Gerbaux, P.; Verbiest, T.; Koeckelberghs, G. Incorporation of Different End Groups in Conjugated Polymers Using Functional Nickel Initiators. *Macromolecules* **2009**, *42* (20), 7638−7641.
(35) Wong, M.; Hollinger, J.; Kozycz, L. M.; McCormick, T. M.; Lu, Y.; Burns, D. C.; Seferos, D. S. An Apparent Size-Exclusion Quantification Limit Reveals a Molecular Weight Limit in the Synthesis of Externally Initiated Polythiophenes. *ACS Macro Lett.* **2012**, *1* (11), 1266−1269.
(36) De Winter, J.; Deshayes, G.; Boon, F.; Coulembier, O.; Dubois, P.; Gerbaux, P. MALDI-ToF Analysis of Polythiophene : Use of Trans −2- [3- (4- T -Butyl-Phenyl) −2-Methyl- 2-Propenylidene] Malononitrile − DCTB − as Matrix. *J. Mass Spectrom.* **2011**, *46*, 237−246.
(37) Sandberg, H. G. O.; Frey, G. L.; Shkunov, M. N.; Sirringhaus, H.; Friend, R. H.; Nielsen, M. M.; Kumpf, C. Ultrathin Regioregular poly(3-Hexyl Thiophene) Field-Effect Transistors. *Langmuir* **2002**, *18* (26), 10176−10182.
(38) Desbief, S.; Hergué, N.; Douhéret, O.; Surin, M.; Dubois, P.; Geerts, Y.; Lazzaroni, R.; Leclère, P. Nanoscale Investigation of the Electrical Properties in Semiconductor Polymer-Carbon Nanotube Hybrid Materials. *Nanoscale* **2012**, *4* (8), 2705−2712.

DOI: 10.1021/acs.macromol.8b01777
Macromolecules XXXX, XXX, XXX−XXX